AD_____

Award Number: W81XWH-12-1-0322

TITLE: Targeting of the MUC1-C Oncoprotein in Colitis-Associated Colorectal Cancer

PRINCIPAL INVESTIGATOR: Kufe, Donald W., M.D.

CONTRACTING ORGANIZATION: Dana-Farber Cancer Institute, Inc
Boston, MA 02115

REPORT DATE: November 2014

TYPE OF REPORT: Final

PREPARED FOR: U.S. Army Medical Research and Materiel Command
Fort Detrick, Maryland 21702-5012

DISTRIBUTION STATEMENT: Approved for Public Release;
Distribution Unlimited

REPORT DOCUMENTATION PAGE

Form Approved
OMB No. 0704-0188

1. REPORT DATE	2. REPORT TYPE	3. DATES COVERED
November 2014	Final Report	14 Aug 2012 - 14 Aug 2014

4. TITLE AND SUBTITLE
Targeting of the MUC1-C Oncoprotein in Colitis-Associated Colorectal Cancer

5a. CONTRACT NUMBER

5b. GRANT NUMBER
W81XWH-12-1-0322

5c. PROGRAM ELEMENT NUMBER

6. AUTHOR(S)
Kufe, Donald, M.D.

E-Mail: donald_kufe@dfci.harvard.edu

5d. PROJECT NUMBER

5e. TASK NUMBER

5f. WORK UNIT NUMBER

7. PERFORMING ORGANIZATION NAME(S) AND ADDRESS(ES)

Dana-Farber Cancer Institute
450 Brookline Avenue
DA 830
Boston, MA 02215-5450

8. PERFORMING ORGANIZATION REPORT NUMBER

9. SPONSORING / MONITORING AGENCY NAME(S) AND ADDRESS(ES)
U.S. Army Medical Research and Materiel Command
Fort Detrick, Maryland 21702-5012

10. SPONSOR/MONITOR'S ACRONYM(S)

11. SPONSOR/MONITOR'S REPORT NUMBER(S)

12. DISTRIBUTION / AVAILABILITY STATEMENT
Approved for Public Release; Distribution Unlimited

13. SUPPLEMENTARY NOTES

14. ABSTRACT
Inflammatory bowel disease (IBD) is associated with the development of colorectal cancer. however, little is known about the mechanisms responsible for the progression of IBD to this malignancy. Our idea is that a better understanding of how IBD progresses to colorectal cancer will provide new insights for drug development against these malignancies.

15. SUBJECT TERMS

16. SECURITY CLASSIFICATION OF:			17. LIMITATION OF ABSTRACT	18. NUMBER OF PAGES	19a. NAME OF RESPONSIBLE PERSON
a. REPORT	b. ABSTRACT	c. THIS PAGE			USAMRMC
U	U	U	UU	17	19b. TELEPHONE NUMBER *(include area code)*

Table of Contents

Targeting of the MUC1-C Oncoprotein in Colitis-Associated Colorectal Cancer
Department of Defense Grant # 10992508
FINAL Progress Report
November 2014

Donald W. Kufe, MD

INTRODUCTION

The **subject** of this project was "colorectal cancer" and the focus area "inflammatory response in the development of colorectal cancer". Inflammatory bowel disease (IBD) is associated with the development of colorectal cancer; however, little is known about the mechanisms responsible for the progression of IBD to malignancy. The **purpose** of the work was to address the hypothesis that aberrant expression of the mucin 1 (MUC1) oncoprotein by chronic intestinal inflammation contributes to the development of colorectal cancers that are in turn dependent on MUC1 for the malignant phenotype. The **scope** of the research was to define the role of MUC1 in the growth and survival of human colon cancer cells growing in vitro and as tumor xenografts in nude mice and to develop a $MUC1^{+}/IL\text{-}10^{-/-}$ model of colitis to determine whether MUC1 function affects the inflammatory response and colon tumorigenesis.

Background. MUC1 is a heterodimeric transmembrane protein that is activated in cytokine-mediated inflammatory responses (1). MUC1 is aberrantly overexpressed in human colon cancers and is associated with invasion, metastases and a poor prognosis (2-8). However, there is limited information regarding a functional role for MUC1 in colon cancer cells.

MUC1 consists of an extracellular N-terminal subunit (MUC1-N) with variable numbers of glycosylated tandem repeats and a C-terminal transmembrane subunit (MUC1-C) (1). MUC1-N is shed from the epithelial cell surface, where it contributes to the intestinal mucosal barrier. In turn, MUC1-C signals growth and survival responses to the interior of cells constituting the epithelial layer (1). The available evidence indicates that colon and other cancer cells have exploited MUC1-C-induced survival signals by aberrantly expressing this subunit. For example, MUC1-C contributes to activation of the WNT/β-catenin pathway, which is frequently activated in colon cancer (9), by binding directly to and stabilizing β-catenin (10). The MUC1-C cytoplasmic domain also interacts directly with TCF7L2/TCF4 and thereby promotes β-catenin/TCF4-mediated transcription of WNT target genes, such as *cyclin D1* (11).

Other studies have linked MUC1-C to the constitutive activation of NF-κB in human carcinomas (12). In this context and like activated NF-κB, MUC1-C contributes to transformation and blocks apoptosis by a mechanism that involves in part upregulation of BCL-XL expression (13, 14). These MUC1-C-induced responses are conferred by interaction of the MUC1-C cytoplasmic domain with the high-molecular weight IκB (IKK) complex (15). In turn, MUC1-C promotes IKKβ activation, resulting in phosphorylation and degradation of IκBα (15). Other work has demonstrated that MUC1-C interacts directly with NF-κB p65 and contributes to activation of NF-κB target genes, such as *BCL-XL* (12). The interaction between MUC1-C and NF-κB has also been linked to the induction of ZEB1, a transcriptional repressor that drives EMT and cancer progression (16).

The transforming growth factor β-activated kinase 1 (TAK1) is a proinflammatory effector that contributes to activation of the IKK complex and thereby the NF-κB pathway (17). TAK1 is a key regulator of the innate immune response and inflammation (17, 18). TAK1 has also been linked to colon cancer cell survival and the control of cell death (19-22). However, little is know about the control of TAK1 levels in inflammation and cancer. Our studies demonstrate that MUC1-C induces TAK1 expression in colon cancer cells. We show that (i) MUC1-C induces TAK1 expression by promoting NF-κB-mediated activation of the TAK1 promoter, and (ii) MUC1-C binds directly to TAK1 and confers the formation of a TAK1 complex with TRAF6, which in turn activates TAK1→NF-κB signaling. In concert with these results, targeting MUC1-C with silencing or with an inhibitor suppresses the TAK1→NF-κB pathway. Our studies extend to a MUC1 transgenic model of inflammatory bowel disease and colon tumorigenesis and provide further support for MUC1-C-mediated induction of TAK1→NF-κB signaling.

BODY

Specific Aim 1: To determine if disrupting MUC1-C function affects the inflammatory response and colon tumorigenesis in a MUC1+/IL-10-/- mouse model of colitis.

Intestinal inflammation increases the risk of developing colon cancer, conceivably through recurrent cycles of damage and repair of the mucosa (23). Aberrant expression of MUC1 protein has been linked to inflammatory bowel disease (24-26); however, to our knowledge, there is no available analysis of MUC1 and its relationship with inflammatory signals in models of colitis and colon tumorigenesis.

Therefore, to develop a mouse model of colitis and tumorigenesis, we first crossed MUC1$^{+/-}$ (here MUC1 represents human MUC1) mice with IL-10$^{-/-}$ mice (obtained from Jackson Laboratories) (Fig. 1A). Genotyping was used for identification of F1 MUC1$^{+/-}$/IL-10$^{+/-}$ mice (Fig. 1B), which were then bred with IL-10$^{-/-}$ mice (Fig. 1A). Results from genotyping the F2 mice demonstrated MUC1$^{+/-}$/IL-10$^{-/-}$ (#1,2,5,6,7,8,10, and 12), MUC1$^{+/-}$/IL-10$^{+/-}$ (#3,4, and 14), and IL-10$^{+/-}$ (#9,11,13 and 15) pups (Fig. 1B).

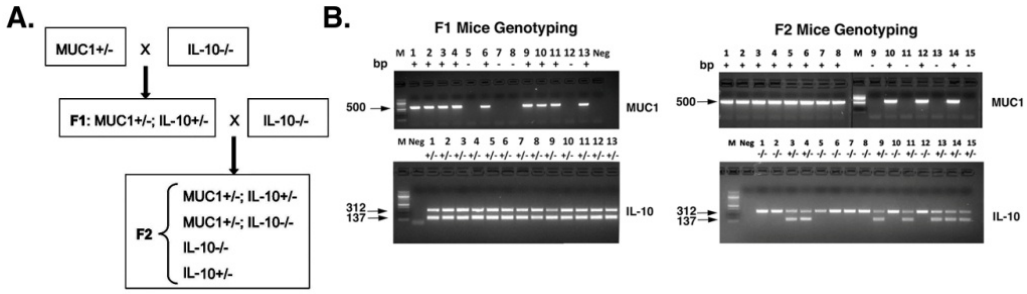

Figure 1. *A. Schema for the breeding strategy of F1 and F2 mice. B. Genotyping of the F1 and F2 pups by PCR for MUC1 and IL-10.*

Mice transgenic for human MUC1 (MUC1$^{+/-}$) that express MUC1 under control of the endogenous human MUC1 promoter exhibit a pattern of expression similar to that found in humans (27). Immunoblot analysis of colon tissue from MUC1$^{+/-}$ mice demonstrated increased MUC1-C levels as compared to that in wild-type mice (Figs. 2A and B). In addition, upregulation of MUC1-C in the MUC1$^{+/-}$ mouse colon was associated with increases in TAK1 and phospho-NF-κB p65 (Figs. 2A and B). BCL-XL levels were also upregulated in colon tissue from the MUC1$^{+/-}$ mouse (Figs. 2A and B).

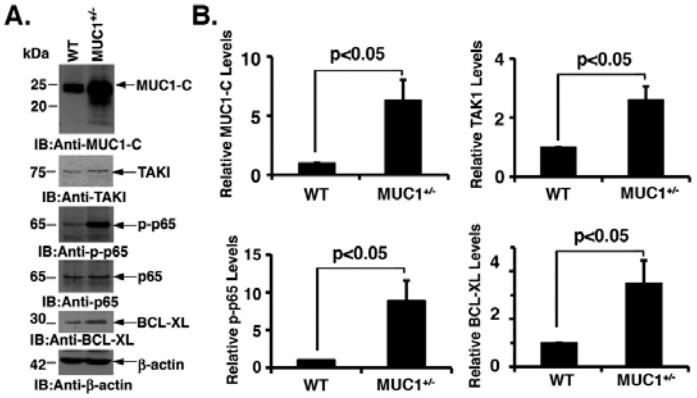

Figure 2. MUC1-C activates TAK1 and NF-κB p65 in mouse colon. *A. Lysates from colon tissue obtained from wild-type (WT) and MUC1$^{+/-}$ mice were immunoblotted with the indicated antibodies. B. Intensities of the MUC1-C, TAK1, p-p65 and BCL-XL signals were quantified using ImageJ software. Results are expressed as relative levels (mean±SD of three independent determinations) as compared to that obtained for colon tissue from WT mice (assigned a value of 1).*

The MUC1$^{+/-}$ mice did not develop colitis as evidenced by a normal colonic mucosa (data not shown). By contrast, IL-10$^{-/-}$ mice develop colitis with epithelial hyperplasia and inflammatory infiltrates due to aberrant regulation of the innate immune response to intestinal flora (28). To assess the effects of MUC1-C on TAK1 signaling in a model of colitis and tumorigenesis (29), we crossed MUC1$^{+/-}$ mice with IL-10$^{-/-}$ mice and then the F1 MUC1$^{+/-}$/IL-10$^{+/-}$ mice were bred with IL-10$^{-/-}$ mice. Analysis of colon tissue from IL-10$^{-/-}$ mice demonstrated marked upregulation of endogenous mouse Muc1-C expression, but at levels somewhat lower than that found in the MUC1$^{+/-}$/IL-10$^{-/-}$ mouse colon (Fig. 3A and B). We also found increases in TAK1, phospho-NF-κB p65 and BCL-XL that were more pronounced in the MUC1$^{+/-}$/IL-10$^{-/-}$ mouse colon (Fig. 3A and B). The presence of colitis as assessed by the development of rectal prolapse supported increased inflammation of the bowel in MUC1$^{+/-}$/IL-10$^{-/-}$, as compared to IL-10$^{-/-}$, mice (Fig. 3C). Moreover, and consistent with previous studies (29), the MUC1$^{+/-}$/IL-10$^{-/-}$ mice exhibited more severe colitis with dysplasia and progression to carcinomas (Fig. 3D).

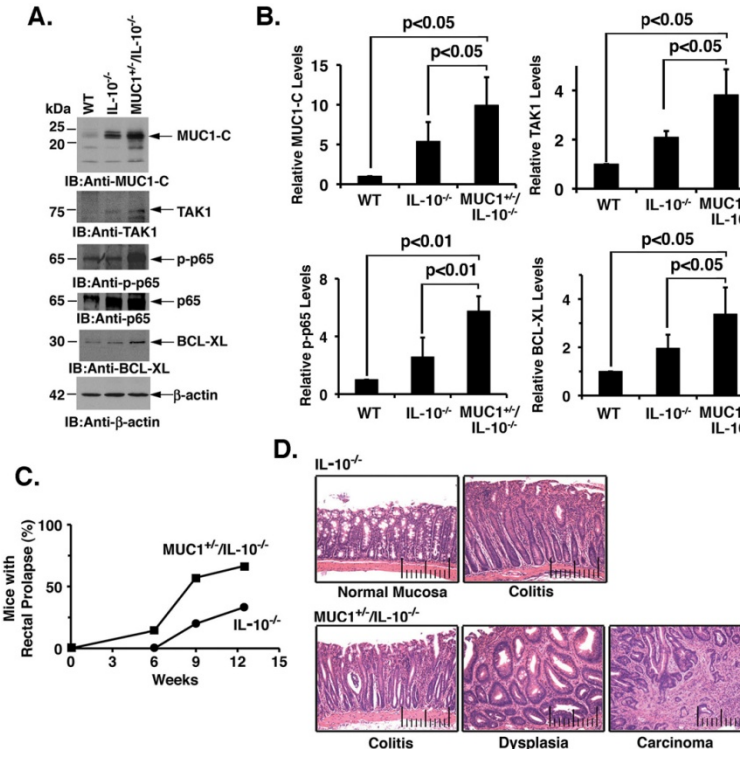

Figure 3. *A. Lysates from colon tissue from WT, IL-10$^{-/-}$ and MUC1$^{+/-}$/IL-10$^{-/-}$ mice were immunoblotted with the indicated antibodies. B. Intensities of the MUC1-C, TAK1, p-p65 and BCL-XL signals were quantified using ImageJ software. Results are expressed as relative levels (mean±SD of three independent determinations) as compared to that obtained for colon tissue from WT mice (assigned a value of 1). C. The percentage of MUC1$^{+/-}$/IL-10$^{-/-}$ (n=7) and IL-10$^{-/-}$ (n=6) mice with rectal prolapse is expressed at the indicated ages. D. Images of colon tissue from IL-10$^{-/-}$ mice (upper panels). The normal mucosa has short straight crypts with very few inflammatory cells between crypts (upper left panel). With the development of colitis, the mucosa is thickened and the crypts are elongated with infiltrates of lymphocytes between the crypts (upper right panel). Images of colon tissue from MUC1$^{+/-}$/IL-10$^{-/-}$ mice (lower panels). Colitis is seen with a thickened mucosa and elongated crypts. Adjacent crypts are separated by infiltrates of inflammatory cells and the presence of crypt abscess (lower left panel). With progression to dysplasia, the crypts are enlarged, twisted and branched with inflammatory cells between the crypts (lower middle panel). The crypts at the top of the image are twisted and tortuous and at the bottom extend into an adenocarcinoma (lower right panel).*

Ongoing studies following completion of funding continue to monitor the MUC1$^{+/-}$/IL-10$^{-/-}$, MUC1$^{+/-}$ and IL-10$^{-/-}$ mice for rectal prolapse and for the development of colon tumors. At that time, additional tissues will be harvested for immunohistochemistry studies. Based on the findings to date, our hypothesis continues to be that MUC1$^{+/-}$/IL-10$^{-/-}$ mice develop colitis at an earlier age than IL-10$^{-/-}$ mice and also develop colon cancer at later stages of inflammation. Our plan will then be to determine whether treatment with GO-203 to disrupt MUC1 function attenuates colitis and colorectal tumor development. Having developed these models with support from the DOD, we will now continue these studies with other funding.

Specific Aim 2: To assess the effects of inhibiting MUC1-C function on activation of the NF-κB, STAT3 and β-catenin pathways that have been linked to colitis and tumorigenesis.

MUC1 has been linked to three major signaling pathways (NF-κB p65, β-catenin and STAT3) associated with intestinal inflammation and colon tumorigenesis (1). Our studies, as described below, focused predominantly on the NF-κB p65 pathway based on the observation that MUC1-C is involved in the regulation of TAK1, which contributes to activation of the IKK complex and NF-κB p65 signaling. Our results also support a model in which MUC1 may contribute in part to inflammation and tumorigenesis through the Wnt/β-catenin, but not the STAT3, pathway.

Silencing MUC1-C decreases TAK1 signaling in colon cancer cells. SK-CO-1 colon cancer cells are dependent on TAK1 for survival (21). MUC1-C was therefore stably silenced in SK-CO-1 cells to determine whether MUC1-C affects TAK1 signaling (Fig. 4A). Notably, silencing MUC1-C in SK-CO-1/MUC1shRNA cells was associated with marked downregulation of TAK1 mRNA levels as compared to that in control SK-CO-1/CshRNA cells (Fig. 4B, left). Silencing MUC1-C was also associated with decreases in TAK1 protein (Fig. 4B, right). In addition, MUC1-C was necessary for activation of phospho-IKKβ and phospho-NF-κB p65 (Fig. 4C, left). Intriguingly, treatment of SK-CO-1 cells with the NF-κB inhibitor BAY11-7085 (30) suppressed TAK1 mRNA levels (data not shown), indicating that MUC1-C may activate a TAK1-NF-κB auto-inductive loop. In concert with these results, silencing MUC1-C decreased activation of a NF-κB p65-driven pGL4.32 promoter-Luc reporter (Fig. 4C, right). To extend this analysis, MUC1-C was downregulated in SW620 colon cancer cells (Fig. 4D). As found with SK-CO-1 cells, MUC1-C suppression in SW620 cells was associated with decreases in TAK1 expression (Fig. 4E, left and right). We also found that silencing of MUC1-

C in SW620 cells results in suppression of NF-κB signaling (Fig. 4F, left and right). These results indicate that MUC1-C contributes to activation of the inflammatory TAK1→NF-κB pathway in colon cancer cells.

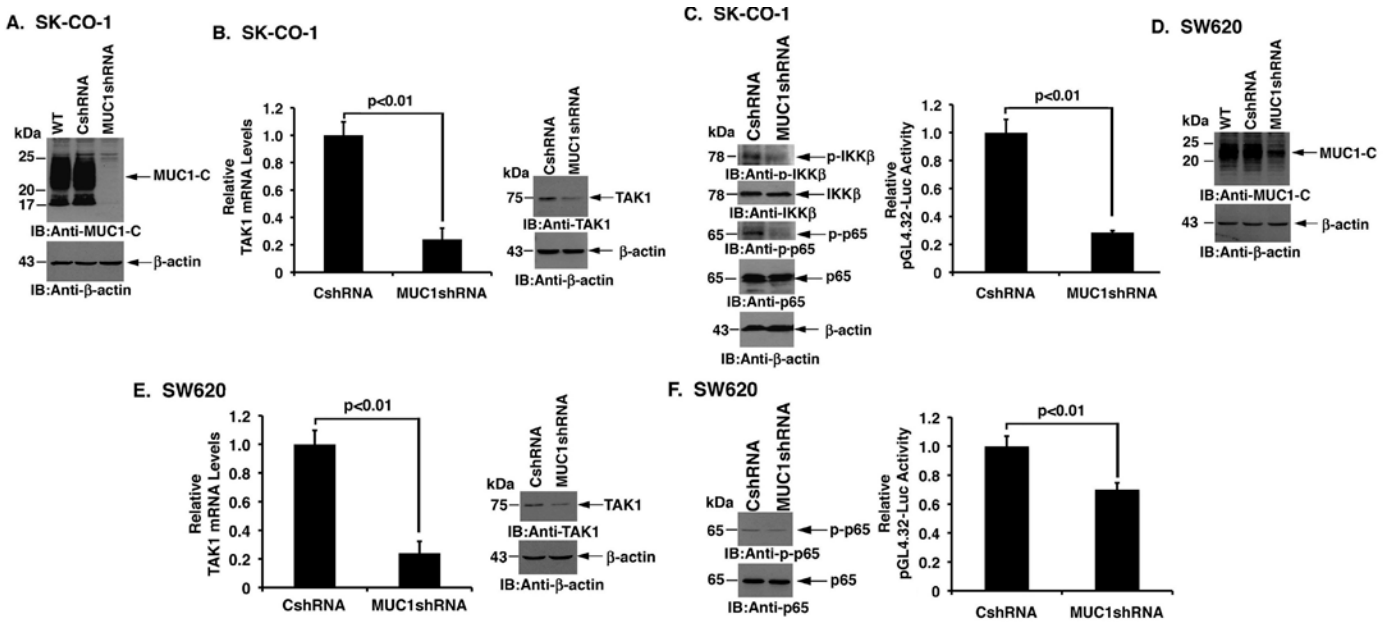

Figure 4. Silencing MUC1-C in KRAS-dependent colon cancer cells suppresses the TAK1→NF-κB pathway. *A. SK-CO-1 cells were infected with lentiviruses to stably express a control CshRNA or a MUC1shRNA. Lysates from the wild-type (WT) and transduced cells were immunoblotted with the indicated antibodies. B. TAK1 mRNA levels in the indicated SK-CO-1 cells were determined by qRT-PCR (left). The results are expressed as relative TAK1 mRNA levels (mean±SD of three determinations) as compared to that obtained for the SK-CO-1/CshRNA cells (left). Lysates were immunoblotted with the indicated antibodies (right). C. Lysates from SK-CO-1/CshRNA and SK-CO-1/MUC1shRNA cells were immunoblotted with the indicated antibodies (left). The indicated cells were transfected with pGL4.32-Luc for 48 h and then assayed for luciferase activity. The results are expressed as the relative luciferase activity (mean±SD of three determinations) compared to that obtained for the SK-CO-1/CshRNA cells (right). D. SW620 cells were infected with lentiviruses to stably express a control CshRNA or a MUC1shRNA. Lysates from the wild-type (WT) and transduced cells were immunoblotted with the indicated antibodies. E. TAK1 mRNA levels in the indicated SW620 cells were determined by qRT-PCR (left). The results are expressed as relative TAK1 mRNA levels (mean±SD of three determinations) as compared to that obtained for the SW620/CshRNA cells (left). Lysates were immunoblotted with the indicated antibodies (right). F. Lysates from the SW620/CshRNA and SW620/MUC1shRNA cells were immunoblotted with the indicated antibodies (left). The indicated cells were transfected with pGL4.32-Luc for 48 h and then assayed for luciferase activity. The results are expressed as the relative luciferase activity (mean±SD of three determinations) compared to that obtained for the SW620/CshRNA cells (right).*

MUC1-C induces TAK1 expression. HCT116 colon cancer cells have low to undetectable levels of MUC1-C as compared to that in SK-CO-1 and SW620 cells. Accordingly, we stably overexpressed MUC1-C in these cells (Fig. 5A) to further define the interaction between MUC1-C and TAK1. In concert with the finding that silencing MUC1-C downregulates TAK1 expression, we found that TAK1 mRNA levels are significantly increased in HCT116/MUC1-C, as compared to HCT116/vector, cells (Fig. 5B, left). Expression of MUC1-C was also associated with increases in TAK1 protein (Fig. 5B, right) and phospho-NF-κB p65 (Fig. 5B, right). Intriguingly, stable silencing of NF-κB p65 in HCT116/MUC1-C cells blocked MUC1-C-induced TAK1 expression (data not shown), providing further support for a potential auto-inductive loop involving MUC1-C, TAK1 and NF-κB. Similarly, in LoVo colon cancer cells transduced to stably overexpress MUC1-C (Fig. 5C), we found increased activation of the TAK1 promoter (Fig. 5D, left) and upregulation of TAK1 mRNA levels (Fig. 5D, right). Expression of MUC1-C was also associated with increases in TAK1 protein and in phospho-NF-κB p65 (Fig. 5E). Consistent with activation of NF-κB p65, expression of MUC1-C in the LoVo cell model resulted in activation of the pGL4.32 promoter-Luc reporter (Fig. 5F). These findings demonstrate that MUC1-C is sufficient for induction of TAK1 and the NF-κB pathway.

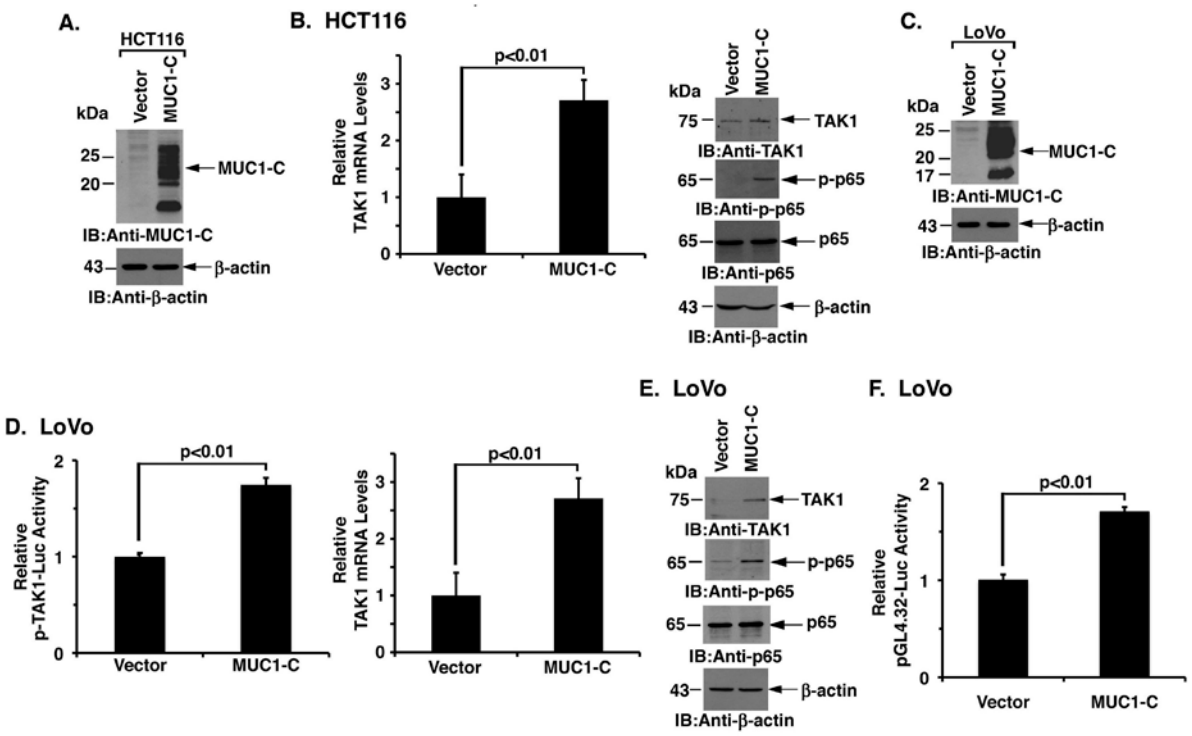

Figure 5. MUC1-C is sufficient for activation of the TAK1→NF-κB pathway. *A. Lysates from HCT116 colon cancer cells transduced to stably express an empty vector or MUC1-C were immunoblotted with the indicated antibodies. B. TAK1 mRNA levels in the indicated HCT116 cells were determined by qRT-PCR (left). The results are expressed as relative TAK1 mRNA levels (mean±SD of three determinations) as compared to that obtained for the HCT116/vector cells (left). Lysates were immunoblotted with the indicated antibodies (right). C. Lysates from LoVo colon cancer cells transduced to stably express an empty vector or MUC1-C were immunoblotted with the indicated antibodies. D. The indicated LoVo cells were transfected with a TAK1 promoter-luciferase reporter (pTAK1-Luc) for 48 h and then assayed for luciferase activity. The results are expressed as the relative luciferase activity (mean±SD of three determinations) compared to that obtained for the LoVo/vector cells (left). qRT-PCR analysis of TAK1 mRNA in the indicated LoVo cells is expressed as relative levels (mean±SD of three determinations) as compared to that obtained for the LoVo/vector cells (right). E. Lysates from the LoVo/vector and LoVo/MUC1-C cells were immunoblotted with the indicated antibodies. F. The indicated LoVo cells were transfected with pGL4.32-Luc for 48 h and then assayed for luciferase activity. The results are expressed as the relative luciferase activity (mean±SD of three determinations) compared to that obtained for the LoVo cells.*

MUC1-C promotes NF-κB p65 occupancy of the TAK1 promoter. Based on the above observations, we searched the human TAK1 (MAP3K7) promoter region using the annotated sequence available at the Ensembl genomic database (ENST00000369329; NCBI Reference Sequence: NG_011966.2) and found a potential NF-κB binding sequence at position -326 to -317 upstream to the transcription start site (Fig. 6A, upper panel). To determine whether this putative NF-κB site contributes to activation of the TAK1 promoter, we compared activation of a wild-type (GGGACCAACC) and mutant (CTCACCAACC) TAK1 promoter-luciferase reporter (pTAK1-Luc) in SK-CO-1 cells. Mutation of the putative NF-κB site was associated with a significant decrease in TAK1 promoter activation (Fig. 6A, lower panel). Based on these results, ChIP studies were performed which demonstrated that NF-κB p65 occupies the TAK1 promoter (Fig. 6B). We also found that silencing MUC1-C in SK-CO-1 cells decreases NF-κB p65 occupancy (Fig. 6B). Re-ChIP analysis further demonstrated that NF-κB p65 occupies the TAK1 promoter with MUC1-C (Fig. 6C). In concert with these findings, activation of the pTAK1-Luc reporter in LoVo/MUC1-C cells was significantly attenuated by mutation of the NF-κB site (Fig. 6D). Moreover, NF-κB p65 occupancy on the TAK1 promoter was increased in LoVo/MUC1-C, as compared to LoVo/vector, cells (Fig. 6E). Re-ChIP studies using the LoVo cells further confirmed that NF-κB occupies the TAK1 promoter with MUC1-C (Fig. 6F). These results collectively provided support for a model in which MUC1-C also promotes NF-κB-mediated activation of TAK1 expression.

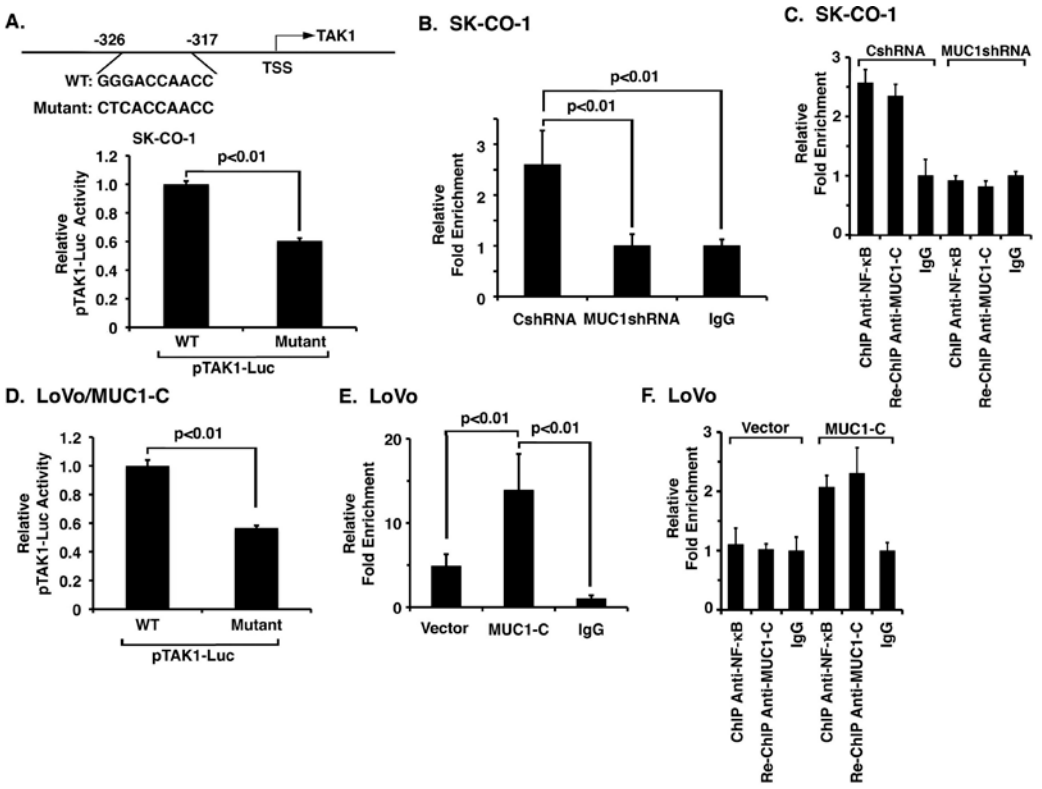

Figure 6. MUC1-C promotes NF-κB-mediated activation of TAK1 expression. *A. Schematic representation of the TAK1 promoter with positioning of the NF-κB binding site (upper panel). SK-CO-1 cells were transfected with wild-type or mutant pTAK1-Luc for 48 h and then assayed for luciferase activity. The results are expressed as the relative luciferase activity (mean±SD of three determinations) compared to that obtained with wild-type pTAK1-Luc (lower panel). B. Soluble chromatin from SK-CO-1/CshRNA and SK-CO-1/MUC1shRNA cells was precipitated with anti-NF-κB p65 and, as a control, IgG. The final DNA samples were amplified by qPCR with pairs of primers for the NF-κB binding region (NBR; -326 to –317). The results (mean±SD of three determinations) are expressed as the relative fold enrichment compared to that obtained with the IgG control. C. Soluble chromatin from the indicated SK-CO-1 cells was precipitated with anti-NF-κB p65. The precipitates were released, reimmunoprecipitated with anti-MUC1-C and then analyzed for TAK1 promoter sequences. The results (mean±SD of three determinations) are expressed as the relative fold enrichment compared to that obtained with the IgG control. D. LoVo/MUC1-C cells were transfected with wild-type or mutant pTAK1-Luc for 48 h and then assayed for luciferase activity. The results are expressed as the relative luciferase activity (mean±SD of three determinations) compared to that obtained with wild-type pTAK1-Luc. E. Soluble chromatin from LoVo/vector and LoVo/MUC1-C cells was precipitated with anti-NF-κB p65 and, as a control, IgG. The final DNA samples were amplified by qPCR with pairs of primers for the NF-κB binding region (NBR). The results (mean±SD of three determinations) are expressed as the relative fold enrichment compared to that obtained with the IgG control. F. Soluble chromatin from the indicated LoVo cells was precipitated with anti-NF-κB p65. The precipitates were released, reimmunoprecipitated with anti-MUC1-C and then analyzed for TAK1 promoter sequences. The results (mean±SD of three determinations) are expressed as the relative fold enrichment compared to that obtained with the IgG control.*

MUC1-C forms a complex with TAK1 and TRAF6. TAK1 phosphorylates IKKβ on Ser-181 and thereby activates the NF-κB pathway (31, 32). The demonstration that MUC1-C associates with IKKβ (15) prompted studies to determine whether MUC1-C also forms a complex with TAK1. Indeed, coimmunoprecipitation (co-IP) experiments using lysates from SK-CO-1 cells showed that MUC1-C associates with TAK1 (Fig. 7A). In concert with these co-IP results and the previous demonstration that MUC1-C interacts with the IKK complex (15), immunodepletion of MUC1-C from SK-CO-1 cell lysates was associated with decreases in TAK1, p-IKKβ and IKKβ (data not shown). As additional controls, MUC1-C/TAK1 complexes were also detectable when co-IP studies were performed on HCT116/MUC1-C, but not HCT116/vector, cell lysates (data not shown). These results collectively supported the association of MUC1-C and TAK1 in cells. In vitro binding studies further demonstrated that the MUC1-C cytoplasmic domain (MUC1-CD; Fig. 7B) interacts directly with GST-TAK1 (Fig. 7C). To define the region of MUC1-CD that confers the interaction, we incubated GST-MUC1-CD deletion mutants with His-TAK1 (Fig. 7D). The results showed that MUC1-CD(1-

45), but not MUC1-CD(46-72), binds to TAK1 (Fig. 7D). We also found that mutation of the MUC1-CD CQC motif to AQA abrogated binding to TAK1 (Fig. 7D), indicating that the Cys residues are of importance for the interaction.

TNF receptor-associated factor 6 (TRAF6) is an E3 ubiquitin ligase that functions upstream to TAK1 and NF-κB activation (33). Based on the known interaction between TAK1 and TRAF6, we asked if, like TAK1, MUC1-C also associates with TRAF6. Indeed, coimmunoprecipitation studies demonstrated that MUC1-C forms a complex with TRAF6 (Fig. 7E, left). In addition, we found that the MUC1-C cytoplasmic domain (MUC1-CD) binds directly to GST-TRAF6 (Fig. 7E, right). However, in contrast to TAK1, the interaction with TRAF6 was conferred by MUC1-CD(20-72) and not MUC1-CD(1-45) (Fig. 7F). The lack of detectable binding of MUC1-CD(46-72) to TRAF6 (Fig. 7F) further supported involvement of a region spanning aa 45-46 and indicated that distinct regions of MUC1-CD bind to TAK1 and TRAF6. Moreover, and in contrast to TAK1, binding to TRAF6 was not affected by mutating MUC1-CD at CQC to AQA (Fig. 7F). The observation that MUC1-CD interacts with both TAK1 and TRAF6 invoked the possibility that MUC1-CD might facilitate the formation of TAK1/TRAF6 complexes. Significantly, there was little if any association of His-TAK1 and GST-TRAF6 in the absence of MUC1-CD (Fig. 7G). By contrast, binding of TAK1 and TRAF6 was clearly observed in the presence of MUC1-CD and this interaction was abrogated by mutation of the CQC motif to AQA (Fig. 7G).

Figure 7. MUC1-C cytoplasmic domain binds directly to TAK1. *A. Lysates from SK-CO-1 cells were precipitated with anti-MUC1-C or a control IgG. The precipitates were immunoblotted with the indicated antibodies. B. Schematic representation of MUC1-C (ED, extracellular domain; TM, transmembrane domain) and the amino acid (aa) sequence of the cytoplasmic domain (CD). Highlighted is the CQC motif that is necessary for MUC1-C homodimerization and has been mutated to AQA in MUC1-CD. C. GST or GST-TAK1 was incubated with purified MUC1-CD. The adsorbates were immunoblotted with anti-MUC1-CD. Input of the GST proteins was assessed by Coomassie blue staining. D. GST, GST-MUC1-CD (full-length; 1-72) or the indicated GST-MUC1-CD mutants were incubated with His-TAK1. The adsorbates were immunoblotted with anti-TAK1. Input of the GST proteins was assessed by Coomassie blue staining. E. Lysates from SK-CO-1 cells were precipitated with anti-MUC1-C or a control IgG. The precipitates were immunoblotted with the indicated antibodies (left). GST or GST-TRAF6 was incubated with purified MUC1-CD. The adsorbates were immunoblotted with anti-MUC1-CD (right). Input of the GST proteins was assessed by Coomassie blue staining (right). F. GST, GST-MUC1-CD(1-72) or the indicated GST-MUC1-CD mutants were incubated with His-TRAF6. The adsorbates were immunoblotted with anti-TRAF6. Input of the GST proteins was assessed by Coomassie blue staining. G. His-TAK1 was incubated with GST or GST-TRAF6 in the presence of MUC1-CD or MUC1-CD(AQA). Adsorbates and input proteins were immunoblotted with the indicated antibodies. Input of the GST-TRAF6 and GST proteins was assessed by Coomassie blue staining.*

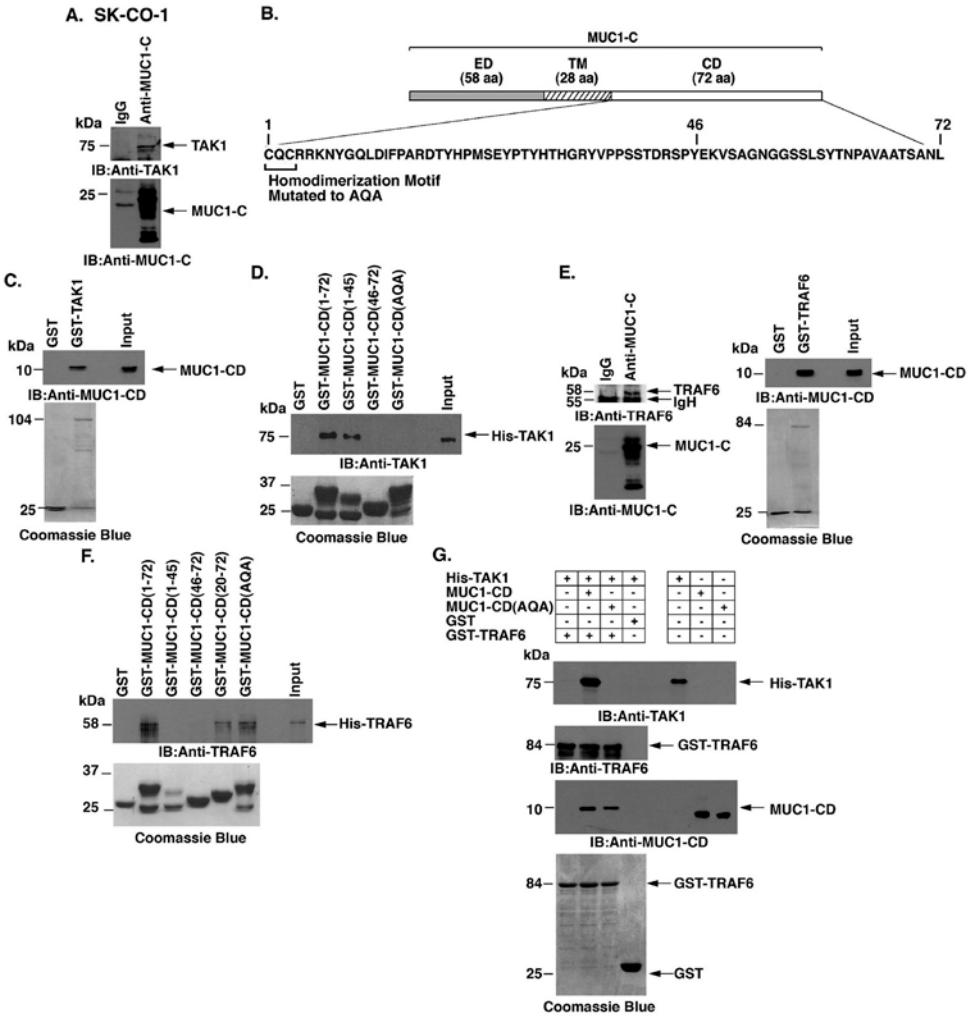

TRAF6 bridges the RAS and NF-κB pathways in lung cancer cells (34); however, little is known about involvement of TRAF6 in colon cancer cells. Of interest in this regard, silencing MUC1-C in SK-CO-1 and SW620 cells was associated with downregulation of TRAF6 mRNA and protein (Figs. 8A and 8B, left and right). Consistent with these results, expression of MUC1-C in HCT116 cells resulted in upregulation of TRAF6 mRNA and protein levels (Fig. 8C, left and right). Moreover, we found that MUC1-C induces TRAF6 expression in LoVo cells (Fig. 8D, left and right), indicating that MUC1-C is sufficient to drive the upregulation of both TAK1 and TRAF6.

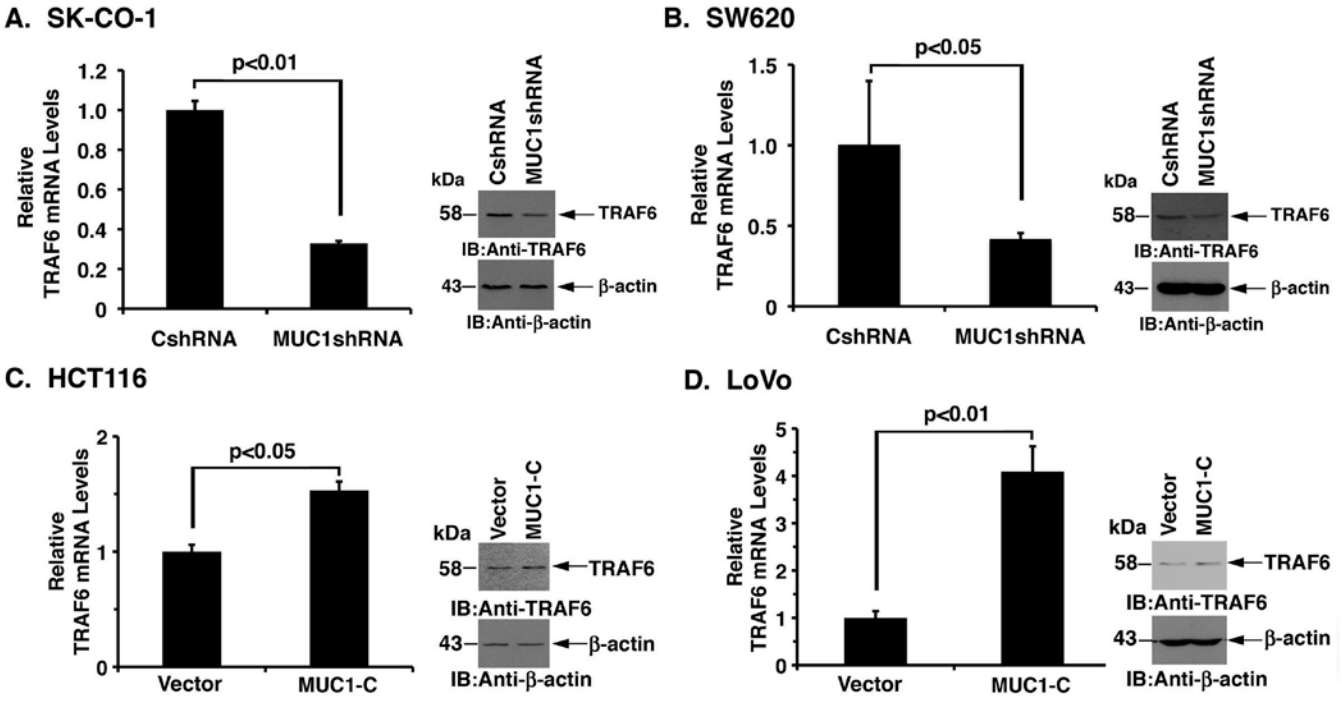

Figure 8. MUC1-C upregulates TRAF6 expression. *A and B. TRAF6 mRNA levels in the indicated SK-CO-1 (A) and SW620 (B) cells were determined by qRT-PCR (left). The results are expressed as relative TRAF6 mRNA levels (mean±SD of three determinations) as compared to that obtained for the CshRNA cells (left). Lysates were immunoblotted with the indicated antibodies (right). C and D. TRAF6 mRNA levels in the indicated HCT116 (C) and LoVo (D) cells were determined by qRT-PCR (left). The results are expressed as relative TRAF6 mRNA levels (mean±SD of three determinations) as compared to that obtained for the vector cells (left). Lysates were immunoblotted with the indicated antibodies (right).*

Specific Aim 3: To define the mechanisms associated with inhibiting MUC1-C that block growth and survival of human colon cancer cells growing in vitro and as xenografts in nude mice.

Targeting the MUC1-C CQC motif blocks TAK1→NF-κB signaling. The findings that MUC1-C induces TAK1 expression and binds directly to TAK1 prompted studies with the cell-penetrating peptide GO-203 that targets the MUC1-C CQC motif and blocks MUC1-C function (35) (Fig. 9A, upper panel). As a control, we used another cell-penetrating peptide, designated CP-2, in which the critical Cys residues for binding to endogenous MUC1-C were mutated to Ala (Fig. 9A, upper panel). Treatment of SK-CO-1 cells with GO-203, but not CP-2, was associated with suppression of TAK1 expression and decreases in NF-κB p65 phosphorylation (Fig. 9A, lower panels). We also found that treatment with GO-203 downregulates expression of the NF-κB target gene, *BCL-XL* (Fig. 9A, lower panels). These effects of GO-203 were conferred, at least in part, by inhibition of NF-κB-mediated transactivation as determined by studies with the pGL4.32 promoter-Luc reporter (Fig. 9B). GO-203 also blocked the interaction between TAK1 and TRAF6 in SK-CO-1 cells (Fig. 9C).

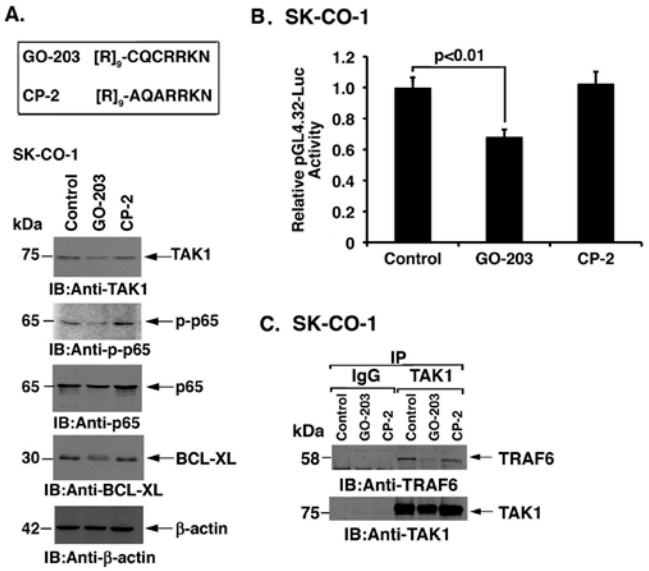

Figure 9. Targeting MUC1-C with GO-203 suppresses TAK1→NF-κB signaling. *A. D-amino acid sequences of the GO-203 and CP-2 peptides (upper panel). SK-CO-1 cells were left untreated or treated with 2.5 μM GO-203 or CP-2 each day for 48 h. Lysates were immunoblotted with the indicated antibodies (lower panels). B. SK-CO-1 cells were transfected with pGL4.32-Luc, treated with 2.5 μM GO-203 or CP-2 each day for 48 h and then assayed for luciferase activity. The results are expressed as the relative luciferase activity (mean±SD of three determinations) compared to that obtained with control untreated cells. C. Lysates from SK-CO-1 cells left untreated or treated with 2.5 μM GO-203 or CP-2 each day for 24 h were precipitated with anti-TAK1. The precipitates were immunoblotted with the indicated antibodies.*

TAK1 contributes to the activation of both (i) NF-κB and (ii) β-catenin/TCF4 signaling in colon cancer cells (21). Accordingly, we asked if targeting MUC1-C and thereby downregulating TAK1 expression also affects the β-catenin/TCF4 pathway. Indeed, silencing MUC1-C in SK-CO-1 and SW620 cells was associated with decreases in activation of the β-catenin/TCF4-driven TOP-Flash promoter-reporter (Figs. 10A and 10B). Silencing MUC1-C was also associated with decreases in AXIN2, the product of a β-catenin/TCF4-dependent target gene (Figs. 10C and 10D), indicating that MUC1-C contributes to activation of the TAK1→NF-κB and β-catenin/TCF4 pathways. Nonetheless, the novelty of a MUC1-C-dependent TAK1 and NF-κB auto-inductive loop that confers upregulation of BCL-XL prompted our focus on that pathway.

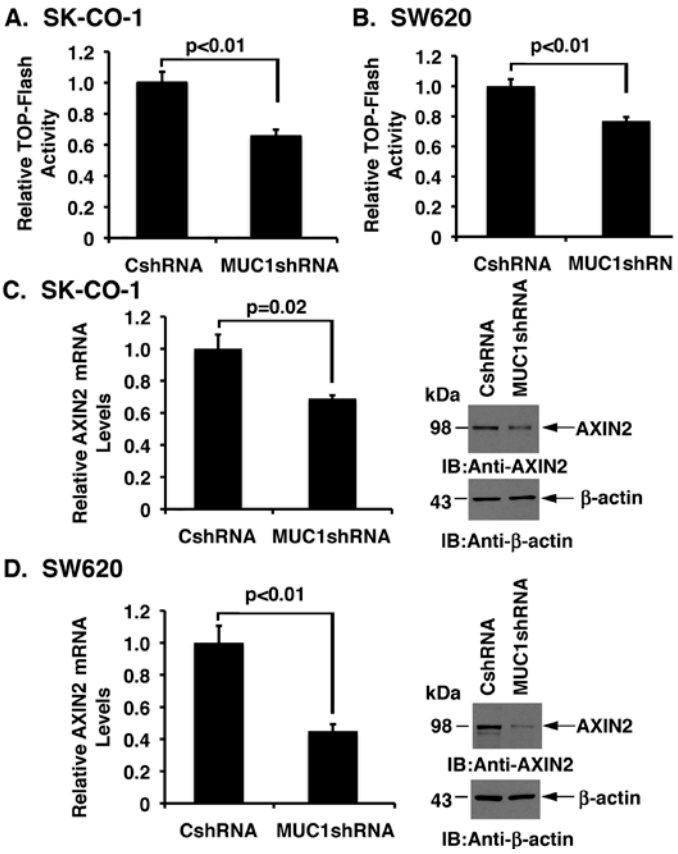

Figure 10. MUC1-C also contributes to activation of β-catenin/TCF4 pathway. *A and B. SK-CO-1 (A) and SW620 (B) cells (1 x 10^5) were seeded into 24-well plates and, after incubation overnight, transfected with TOPFlash or FOPFlash and SV-40-Renilla-Luc in the presence of Lipofectamine LTX. At 48 h after transfection, cells were lysed in passive lysis buffer and luciferase activity was measured using the Dual-Luciferase Reporter Assay System (Promega). The results are expressed as the relative luciferase activity (mean±SD of three determinations) compared to that obtained with FOPFlash. C and D. AXIN2 mRNA levels in the indicated SK-CO-1 (C) and SW620 (D) cells were determined by qRT-PCR (left). The results are expressed as relative TAK1 mRNA levels (mean±SD of three determinations) as compared to that obtained for the CshRNA cells (left). Lysates from the indicated SK-CO-1 (C) and SW620 (D) cells were immunoblotted with anti-AXIN2 and anti-β-actin (right).*

To further assess the effects of targeting MUC1-C, MUC1-positive SK-CO-1 (Fig. 11A), COLO-205 (Fig. 11B) and COLO-320 (Fig. 11C) colorectal cancer cells were left untreated (Control) and treated with 2.5 μM GO-203 or CP-2 for the indicated times. Treatment with GO-203 was associated with inhibition of growth and loss of survival (late apoptosis/necrosis) (Figs. 11A-C). By contrast, the control CP-2 peptide had little if any effect (Figs. 11A-C). In addition, treatment of MUC1-negative HCT116 colon cancer cells with GO-203 was ineffective in inhibiting growth (Fig. 11D). These findings demonstrate that human colorectal cancer cells that express MUC1 are dependent on MUC1-C for their growth and survival.

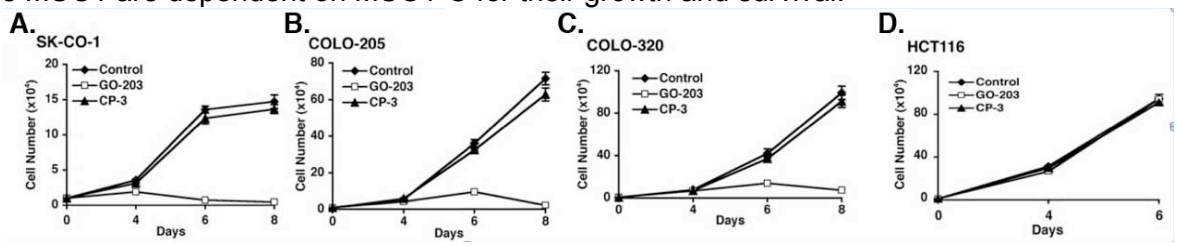

Figure 11. Targeting MUC1-C with GO-203 in colorectal cancer cell lines growing in vitro. *A-D. SK-CO-1 (B; MUC1-positive), COLO-205 (C; MUC1-positive), COLO-320 (D; MUC1-positive), and HCT116 (E; MUC1-negative) cells were left untreated (Control) and treated with 2.5 μM GO-203 or CP-3 for the indicated times. Viable cell number was determined by trypan blue staining.*

Previous studies demonstrated that MEK inhibitors are highly effective against KRAS mutant cancers when combined with agents that target BCL-XL (36). Therefore, based on the finding that GO-203 decreases BCL-XL, we treated SK-CO-1 cells with GO-203 in combination with the MEK inhibitor AS703026. Inhibitory effects of the GO-203+AS703026 combination on SK-CO-1 colony formation were more pronounced than with either agent alone (Fig. 12A, upper panel). Moreover, isobologram analysis of the combination showed marked synergy with a combination index of less than 0.1 (Fig. 12A, lower panels; Table 1). Similar results were obtained when GO-203 was combined with the MEK inhibitor GSK1120212 (Fig. 12B, upper and lower panels; Table 1). These findings with SK-CO-1 cells were confirmed when SW620 cells were treated with the combination of GO-203 and MEK inhibitors (Figs. 12C and D; Table 1), indicating that GO-203 is synergistic with different MEK inhibitors.

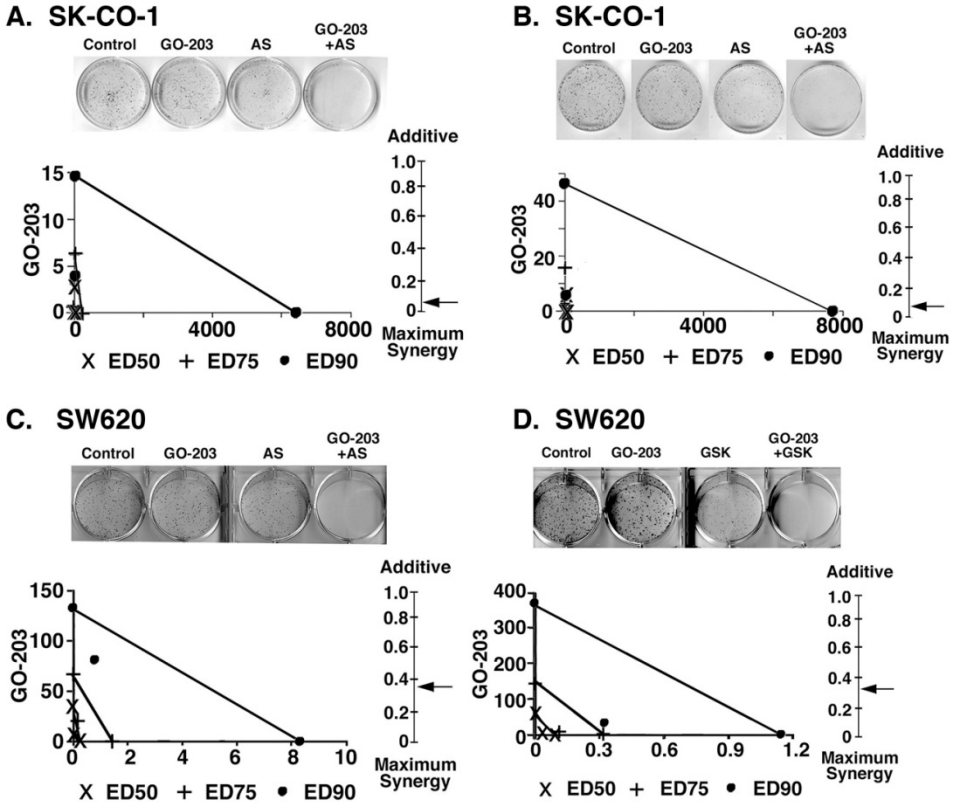

Figure 12. Targeting MUC1-C with GO-203 is synergistic with MEK inhibitors. *A. SK-CO-1 cells were left untreated (solid diamonds) and treated with 2.5 μM GO-203 (open squares) or CP-2 (solid triangles) each day for the indicated days. Viable cell number (mean±SD of three replicates) was determined by trypan blue staining. B. SK-CO-1 cells were seeded at 100 cells/well in 6-well plates and left untreated (Control) or treated each day with 0.61 μM GO-203 alone, 1.17 μM AS703026 alone on day 0, or the GO-203/AS703026 combination for 3 d. Colonies were stained with crystal violet on day 14 after treatment (upper panel). SK-CO-1 cells were treated with (i) fixed IC50 ratios of GO-203 alone on days 0, 1, 2 and 3, (ii) fixed IC50 ratios of AS703026 alone on day 0, and (iii) the GO-203/AS703026 combination for 4 d. The multiple effect isobologram analyses on day 4 are shown for the ED50 (X), ED75 (+) and ED90 (o) values (lower left panel). The combination index (CI) is indicated with the arrow (lower right panel). F. SK-CO-1 cells were seeded at 100 cells/well in 6-well plates and left untreated (Control) or treated each day with 1.22 μM GO-203 alone, 9.63 nM GSK1120212 alone on day 0, or the GO-203/GSK1120212 combination for 3 d. Colonies were stained with crystal violet on day 14 after treatment (upper panel). SK-CO-1 cells were treated with (i) fixed IC50 ratios of GO-203 alone on days 0, 1, 2 and 3, (ii) fixed IC50 ratios of GSK1120212 alone on day 0, and (iii) the GO-203/GSK1120212 combination for 4 d. The multiple effect isobologram analyses on day 4 are shown for the ED50 (X), ED75 (+) and ED90 (o) values (lower left panel). The combination index (CI) is indicated with the arrow (lower right panel). CI values are included in Table 1. C. SW620 cells were seeded at 100 cells/well in 6-well plates and left untreated (Control) or treated each day with 5.2 μM GO-203 alone, 52 nM AS703026 alone on day 0, or the GO-203/AS703026 combination for 3 d. Colonies were stained with crystal violet on day 14 after treatment (upper panel). SW620 cells were treated with (i) fixed IC50 ratios of GO-203 alone on days 0, 1, 2 and 3, (ii) fixed IC50 ratios of AS703026 alone on day 0, and (iii) the GO-203/AS703026 combination for 4 d. The multiple effect isobologram analyses on day 4 are shown for the ED50 (X), ED75 (+) and ED90 (o) values (lower left panel). The combination index (CI) is indicated with the arrow (lower right panel). D. SW620 cells were seeded at 100 cells/well in 6-well plates and left untreated (Control) or treated each day with 5.2 μM GO-203 alone, 52 nM GSK1120212 alone on day 0, or the GO-203/GSK1120212 combination for 3 d. Colonies were stained with crystal violet on day 14 after treatment (upper panel). SW620 cells were treated with (i) fixed IC50 ratios of GO-203 alone on days 0, 1, 2 and 3, (ii) fixed IC50 ratios of GSK1120212 alone on day 0, and (iii) the GO-203/GSK1120212 combination for 4 d. The multiple effect isobologram analyses on day 4 are shown for the ED50 (X), ED75 (+) and ED90 (o) values (lower left panel). The combination index (CI) is indicated with the arrow (lower right panel). CI values are included in Table 1.*

Table 1. Combination Index Values

CI value for GO-203 and AS703026			
Cell line	**ED50**	**ED75**	**ED90**
SK-CO-1	0.05763	0.08882	0.25851
SW620	0.26281	0.18489	0.14103
CI value for GO-203 and GSK1120212			
Cell line	**ED50**	**ED75**	**ED90**
SK-CO-1	0.35792	0.44497	0.70404
SW620	0.43887	0.40064	0.37294

To extend these results obtained from in vitro experiments, we established subcutaneous COLO-205 colon tumor xenografts (~90 mm^3) in the flanks of nude mice. Groups of 8 mice each were treated intraperitoneally (ip) with PBS (Control), 18 mg/kg GO-203, or 18 mg/kg CP-3 each day for 28 days (Fig. 13A). Compared to the control group, growth of the COLO-205 tumors was inhibited in the GO-203-treated mice (Fig. 13A). Moreover, these tumors regressed completely by the end of treatment (day 28) and there was no evidence for regrowth by day 180 (Fig. 13A). In contrast to the anti-tumor activity of GO-203, treatment with CP-3 had no effect on COLO-205 tumor growth (Fig. 13A). Importantly, GO-203 was not associated with loss of body weight or other apparent toxicities. Studies were also performed on established subcutaneous SK-CO-1 tumor xenosgrafts (~90 mm^3) to explore other GO-203 dose-schedules (Fig. 13B). Groups of 8 mice each

were treated with PBS (Control), 6 mg/kg GO-203 each day for 5 days intravenously (iv), or 3 mg/kg GO-203 each day for 5 days iv each week for two weeks. The results demonstrate that, as compared to the control group, growth of tumors in the mice treated with GO-203 was inhibited with both dose-schedules (Fig. 13B). These findings indicate that GO-203 is effective in inhibiting growth and survival of MUC1-positive colorectal cancer cells in mouse xenograft models. The findings also support a GO-203 dose-response effect with regression of tumors at higher doses (18 mg/kg) administered for longer periods (28 days).

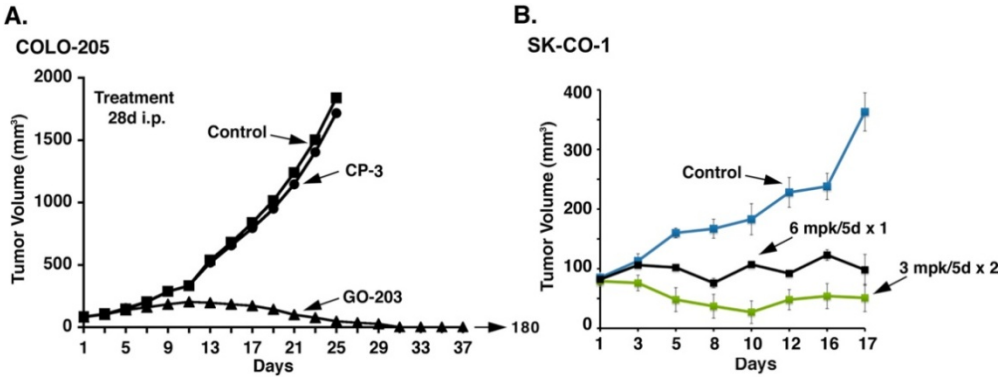

Figure 13. GO-203 is effective against COLO-205 and SK-CO-1 colon cancer xenografts growing in nude mice. *A and B. BALB/c nu/nu mice were injected subcutaneously in the flank with 1 x 10^7 COLO-205 (A) or SK-CO-1 (B) cells. The mice were pair matched when the tumors were ~100 mm^3. A. Treatment groups consisted of 8 mice injected intraperitoneally (ip) with PBS (vehicle control), 18 mg/kg GO-203 or 18 mg/kg CP-3 each day for 28 days. B. Treatment groups consisted of 8 mice injected iv with PBS, 6 mg/kg GO-203 each day for 5 days, or 3 mg/kg GO-203 each day for 5 days each week for 2 weeks. Tumor measurements were performed as indicated and mice were weighed twice weekly. There was no weight loss in any of the groups. The results are expressed as the mean tumor volume with a SE of less than 20%.*

KEY RESEARCH ACCOMPLISHMENTS

The key research accomplishments emanating from this research are that: (1) the MUC1-C oncoprotein induces expression of TAK1, an essential effector of inflammation, in human colon cancer cells; (2) MUC1-C also induces TAK1 and thereby the proinflammatory NF-κB pathway in a transgenic mouse model of MUC1-driven colitis and colon tumorigenesis; (3) MUC1-C promotes NF-κB-mediated activation of TAK1 transcription and, in a positive regulatory loop, MUC1-C contributes to TAK1-induced NF-κB signaling (Fig. 14); (4) MUC1-C binds directly to TAK1 and confers the association of TAK1 with TRAF6, which is necessary for TAK1-mediated activation (Fig. 14); (5) targeting MUC1-C with the GO-203 inhibitor suppresses the TAK1→NF-κB pathway and thereby downregulates BCL-XL; and (6) GO-203 is synergistic with MEK inhibitors in the treatment of colon cancer cells; and (7) targeting MUC1-C with GO-203 inhibits growth of MUC1-positive colon cancer cells growing in vitro and as xenografts in mice. These findings collectively support the importance of MUC1-C in activation of the TAK1→NF-κB pathway in promoting intestinal inflammation and colon cancer progression.

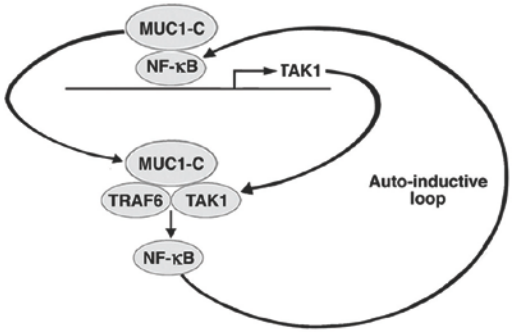

Figure 14. *Schema depicting the proposed MUC1-C-mediated auto-inductive loop involving activation of TAK1 and NF-κB. MUC1-C promotes NF-κB-mediated induction of TAK1 transcription by interacting with NF-κB p65 on the TAK1 promoter and increasing NF-κB occupancy. MUC1-C also forms a complex with TAK1 that can facilitate binding of TAK1 and TRAF6, which is necessary for activation of the downstream NF-κB pathway. In a positive regulatory loop, activated NF-κB interacts with MUC1-C and drives TAK1 expression. In turn, MUC1-C contributes to intestinal inflammation and colon cancer.*

REPORTABLE OUTCOMES

There are no reportable outcomes to date from this research funding. A manuscript describing these results is now under review for publication.

CONCLUSION

Our results provide the first evidence that MUC1-C (i) is of importance mechanistically to the link between intestinal inflammation and colon cancer progression and (ii) represents an attractive target for the treatment of colon cancer.

REFERENCES

1. Kufe, D, *Mucins in cancer: function, prognosis and therapy.* Nature Reviews Cancer, 2009. 9:874-85.
2. Byrd, JC and Bresalier RS, *Mucins and mucin binding proteins in colorectal cancer.* Cancer Metastasis Rev, 2004. 23:77-99.
3. Suzuki, H, et al., *Expression of MUC1 recognized by monoclonal antibody MY.1E12 is a useful biomarker for tumor aggressiveness of advanced colon carcinoma.* Clin Exp Metastasissis, 2004. 21:321-9.
4. Niv, Y, *MUC1 and colorectal cancer pathophysiology considerations.* World J Gastroenterol, 2008. 14:2139-41.
5. Lugli, A, et al., *Prognostic significance of mucins in colorectal cancer with different DNA mismatch-repair status.* J Clin Pathol, 2007. 60:534-9.
6. Nakamori, S, et al., *MUC1 mucin expression as a marker of progression and metastasis of human colorectal carcinoma.* Gastroenterology, 1994. 106:353-61.
7. Baldus, SE, et al., *Comparative evaluation of the prognostic value of MUC1, MUC2, sialyl-Lewis(a) and sialyl-Lewis(x) antigens in colorectal adenocarcinoma.* Histopathology, 2002. 40:440-9.
8. Duncan, TJ, et al., *The role of MUC1 and MUC3 in the biology and prognosis of colorectal cancer.* World J Surg Oncol, 2007. 5:31.
9. Fearon, ER, *Molecular genetics of colorectal cancer.* Annu Rev Pathol, 2011. 6:479-507.
10. Huang, L, et al., *MUC1 oncoprotein blocks GSK3β-mediated phosphorylation and degradation of β-catenin.* Cancer Res, 2005. 65:10413-22.
11. Rajabi, H, et al., *MUC1-C oncoprotein induces TCF7L2 activation and promotes cyclin D1 expression in human breast cancer cells.* J Biol Chem, 2012. 287:10703-13.
12. Ahmad, R, et al., *MUC1-C oncoprotein functions as a direct activator of the NF-κB p65 transcription factor.* Cancer Res, 2009. 69:7013-21.
13. Li, Y, et al., *Human DF3/MUC1 carcinoma-associated protein functions as an oncogene.* Oncogene, 2003. 22:6107-10.
14. Raina, D, et al., *The MUC1 oncoprotein activates the anti-apoptotic PI3K/Akt and Bcl-xL pathways in rat 3Y1 fibroblasts.* J Biol Chem, 2004. 279:20607-12.
15. Ahmad, R, et al., *MUC1 oncoprotein activates the IκB kinase β complex and constitutive NF-κB signaling.* Nat Cell Biol, 2007. 9:1419-27.
16. Rajabi, H, et al., *MUC1-C oncoprotein activates the ZEB1/miR-200c regulatory loop and epithelial-mesenchymal transition.* Oncogene, 2013. 33:1680-9.
17. Sakurai, H, *Targeting of TAK1 in inflammatory disorders and cancer.* Trends Pharmacol Sci, 2012. 33:522-30.
18. Ajibade, AA, et al., *Cell type-specific function of TAK1 in innate immune signaling.* Trends Immunol, 2013. 34:307-16.
19. Omori, E, et al., *Ablation of TAK1 upregulates reactive oxygen species and selectively kills tumor cells.* Cancer Res, 2010. 70:8417-25.
20. Ray, DM, et al., *Inhibition of transforming growth factor-beta-activated kinase-1 blocks cancer cell adhesion, invasion, and metastasis.* Br J Cancer, 2012. 107:129-36.
21. Singh, A, et al., *TAK1 inhibition promotes apoptosis in KRAS-dependent colon cancers.* Cell, 2012. 148:639-50.
22. Mihaly, SR, et al., *TAK1 control of cell death.* Cell Death Differ, 2014. 21:1667-76.
23. Ullman, TA and Itzkowitz SH, *Intestinal inflammation and cancer.* Gastroenterology, 2011. 140:1807-16.

24. Campbell, BJ, et al., *Altered glycosylation in inflammatory bowel disease: a possible role in cancer development.* Glycoconj J, 2001. 18:851-8.
25. Rhodes, JM, *Unifying hypothesis for inflammatory bowel disease and associated colon cancer: sticking the pieces together with sugar.* Lancet, 1996. 347:40-4.
26. Furr, AE, et al., *Aberrant expression of MUC1 mucin in pediatric inflammatory bowel disease.* Pediatr Dev Pathol, 2010. 13:24-31.
27. Rowse, GJ, et al., *Tolerance and immunity to MUC1 in a human MUC1 transgenic murine model.* Cancer Res, 1998. 58:315-21.
28. Berg, DJ, et al., *Enterocolitis and colon cancer in interleukin-10-deficient mice are associated with aberrant cytokine production and CD4(+) TH1-like responses.* J Clin Invest, 1996. 98:1010-20.
29. Beatty, PL, et al., *Cutting edge: transgenic expression of human MUC1 in IL-10-/- mice accelerates inflammatory bowel disease and progression to colon cancer.* J Immunol, 2007. 179:735-9.
30. Relic, B, et al., *15-deoxy-delta12,14-prostaglandin J2 inhibits Bay 11-7085-induced sustained extracellular signal-regulated kinase phosphorylation and apoptosis in human articular chondrocytes and synovial fibroblasts.* J Biol Chem, 2004. 279:22399-403.
31. Wang, C, et al., *TAK1 is a ubiquitin-dependent kinase of MKK and IKK.* Nature, 2001. 412:346-51.
32. Takaesu, G, et al., *TAK1 is critical for IkappaB kinase-mediated activation of the NF-kappaB pathway.* J Mol Biol, 2003. 326:105-15.
33. Yamazaki, K, et al., *Two mechanistically and temporally distinct NF-kappaB activation pathways in IL-1 signaling.* Sci Signal, 2009. 2:ra66.
34. Starczynowski, DT, et al., *TRAF6 is an amplified oncogene bridging the RAS and NF-kappaB pathways in human lung cancer.* J Clin Invest, 2011. 121:4095-105.
35. Raina, D, et al., *Targeting cysteine-mediated dimerization of the MUC1-C oncoprotein in human cancer cells.* Int J Oncol, 2012. 40:1643-9.
36. Corcoran, RB, et al., *Synthetic lethal interaction of combined BCL-XL and MEK inhibition promotes tumor regressions in KRAS mutant cancer models.* Cancer Cell, 2013. 23:121-8

APPENDICES

None.

SUPPORTING DATA

The figures and their legends have been incorporated into the above text.

.